J. Eukaryot. Microbiol., 56(1), 2009 pp. 88–103

DOI: 10.1111/j.1550-7408.2008.00378.x

Sexual and Asexual Processes in *Protoperidinium steidingerae* Balech (Dinophyceae), with Observations on Life-History Stages of *Protoperidinium depressum* (Bailey) Balech (Dinophyceae)

KRISTIN E. GRIBBLE,[a] DONALD M. ANDERSON[a] and D. WAYNE COATS[b]

[a]*Biology Department, Woods Hole Oceanographic Institution, Woods Hole, Massachusetts 02543, and*
[b]*Smithsonian Environmental Research Center, PO Box 28, Edgewater, Maryland 21037*

ABSTRACT. A suite of morphological, histological, and molecular techniques was used to reveal for the first time division, sexuality, mandatory dormancy period of hypnozygotes, and identity of life-history stages of any *Protoperidinium* spp. In both *Protoperidinium steidingerae* and *Protoperidinium depressum*, asexual division occurred by eleutheroschisis within a temporary cyst, yielding two daughter cells. Daughter cells were initially round and one-half to two-thirds the size of parent cells then rapidly increased in size, forming horns before separating. Gamete production and fusion was constitutive in clonal and non-clonal cultures, indicating that both species may be homothallic. Gametes were isogamous, approximately half the size and lacking the pink pigmentation of the vegetative cells, and were never observed to feed. Gamete fusion resulted in a planozygote with two longitudinal flagella. Planozygotes of *P. steidingerae* formed hypnozygotes. The fate of planozygotes of *P. depressum* is unknown. Hypnozygotes of *P. steidingerae* had a mandatory dormancy period of ca. 70 days. Germination resulted in planomeiocytes with two longitudinal flagella. Nuclear cyclosis occurred in the planozygotes of *P. depressum*, but in the planomeiocytes of *P. steidingerae*. The plate tabulation and gross morphology of gametes of *P. steidingerae* and *P. depressum* differed markedly from those of vegetative cells. Thus, misidentification of morphologically distinct life-history stages and incomplete examination of thecal plate morphology in field specimens has likely led to taxonomic confusion of *Protoperidinium* spp. in previous studies.

Key Words. Eleutheroschisis, gamete, heterotrophic dinoflagellate, hypnozygote, nuclear cyclosis, planomeiocyte, planozygote.

PROTOPERIDINIUM Bergh is a cosmopolitan genus of heterotrophic, thecate, marine dinoflagellates with more than 200 described species (Balech 1974). *Protoperidinium* species are raptorial with digestion external to the theca, allowing consumption of large phytoplankton, including diatoms and dinoflagellates (Gaines and Taylor 1984; Jacobson and Anderson 1986; Naustvoll 2000) and even zooplankton eggs and nauplii (Jeong 1996). Although the subject of extensive taxonomic investigation for more than 120 years, the many, diverse species encountered in field studies are often collectively described and enumerated as ''*Protoperidinium* spp.,'' as species identification requires detailed examination of thecal plate morphology. In the past 20 years, several laboratory studies have addressed the feeding mechanisms, grazing rates, preferred foods, and growth rates of a few *Protoperidinium* spp. (Buskey, Coulter, and Brown 1994; Jacobson and Anderson 1986, 1993; Jeong and Latz 1994; Menden-Deuer et al. 2005). Because culturing these heterotrophs is difficult and labor intensive, little else is known about the autecology of members of the genus.

There is currently no information about how conserved the life-cycle characteristics might be among species in this large and diverse genus. Dormant cysts (hypnozygotes) have been identified for many *Protoperidinium* species, indicating the possible presence of a sexual cycle in at least some species. Such cyst–theca relationships have been established by germination in the laboratory of cysts collected in the field. Hypnozygotes have not been identified for all species; it may be that some species do not form dormant cysts during the sexual cycle or that not all species have a sexual cycle. The remainder of the life cycle, including the process of asexual reproduction, remains undescribed for all *Protoperidinium* spp.

The life history of *Protoperidinium steidingerae* Balech and life-cycle stages of *Protoperidinium depressum* (Bailey) Balech presented here provide the first account of asexual and sexual cycles for any species of *Protoperidinium*. In this study, life-cycle stages of *P. steidingerae* and *P. depressum* were examined using cultures isolated from Vineyard Sound off the coast of Woods Hole, MA and from the northeast Atlantic off the western coast of Ireland, respectively. Asexual division, gamete morphology and fusion, mandatory dormancy and germination rates of hypnozygotes, and the identity of other morphologically distinct life-history stages were revealed using a suite of morphological and molecular tools.

Corresponding Author: K. Gribble, Marine Biological Laboratory, 7 MBL St., Lillie 319, Woods Hole, Massachusetts 02543 USA—Telephone number: 508-289-7194; FAX number: 508-457-4727; e-mail: kgribble@mbl.edu

MATERIALS AND METHODS

***Protoperidinium* cultures.** Two non-clonal strains of *P. steidingerae* were isolated from Vineyard Sound, Woods Hole, MA: MV0923-PO-1 in September of 2004 and MV0802 in August 2005. From MV0923-PO-1, two clonal cultures were later established (MV0923-PO-1-Clone6 and MV0923-PO-1-Clone7). *Protoperidinium steidingerae* cultures were maintained in 0.2 µm-filtered, autoclaved seawater of 30 psu (practical salinity units) from Vineyard Sound, with a mixture of *Ditylum brightwellii* (West) Grunow (CCMP 356) and *Chaetoceros affinis* Lauder (CCMP 158) as prey. Cultures were maintained in 70-ml tissue culture flasks (Falcon, 353009, Becton Dickinson, Franklin Lakes, NJ) without air space and were rotated on a plankton wheel at 1–2 rpm at 15 °C under low light (i.e. 50 µmol photon/m^2/s) on a 14 h:10 h light:dark cycle. Transfers were made every 4–5 days by pouring approximately two-thirds the volume of the old culture into a new flask containing fresh sterile-filtered seawater, 4 ml of *D. brightwellii* (ca. 25,000 cells/ml), and 3 ml of *C. affinis* (ca. 400,000 cells/ml).

A clonal strain of *P. depressum* (PDIR1A-Clone 1) was isolated from the northeast Atlantic Ocean off the western coast of Ireland in July of 2002. *Protoperidinium depressum* cultures were maintained as above for *P. steidingerae*, except that cells were grown in Vineyard Sound seawater amended to 35 psu by evaporation and were fed a mixture of *D. brightwellii* (West) Grunow (CCMP 356), *Chaetoceros affinis* Lauder (CCMP 158), and *Lingulodinium polyedrum* (Stein) Dodge (GPES22).

Phytoplankton cultures. Diatom cultures used as prey were grown as described in Gribble and Anderson (2006). In brief, *D. brightwellii* (CCMP 356) and *C. affinis* (CCMP158) cultures were maintained in tubes with 25 ml of *f*/2 nutrient medium plus silicate (Guillard 1975) at 15 °C. Cultures of the dinoflagellate

L. polyedrum (GPES 22) were maintained in 25 ml of ES nutrient medium (Kokinos and Anderson 1995) at 20 °C. All prey cultures were kept at a photon flux density of ca. 100 μmol/m^2/s on a 14 h:10 h light:dark cycle.

Species identification. Morphological species identification for *P. steidingerae* and *P. depressum* was confirmed by examination of thecal plate structure using scanning electron microscopy (SEM) alone or in combination with Calcofluor White MR2 (Polysciences, Warrington, PA) to visualize the cellulose thecal plates (Fritz and Triemer 1985). Samples from culture were preserved with either 5% borate-buffered formalin (v/v, final concentration, *P. steidingerae*) or 4% gluteraldhyde (v/v, final concentration, *P. depressum*) and stored at 4 °C until processed for SEM. For each *Protoperidinium* species, several hundred cells were isolated by micropipette, pooled, and drawn down onto filters (nucleopore membrane, 13 mm, 5-μm pore size, or 25 mm, 8-μm pore size). Cells on filters were rinsed with filtered seawater, 50%:50% filtered seawater:deionized (DI) water (*P. depressum* only), and then DI water before dehydration in a series of ethanol washes of increasing concentration. Following ethanol dehydration, specimens were critical point dried (Tousimis Samdri-780A, Tousimis Research Corp., Rockville, MD), sputter coated with gold palladium (Tousimis Samsputter-28, Tousimis Research Corp., Rockville, MD), and examined on a JEOL JSM-840 SEM (Tokyo, Japan).

For epifluorescence microscopy, samples were preserved with 5% formalin (v/v, final concentration) and stored at 4 °C until processed. Samples were centrifuged, aspirated to a pellet, resuspended in 1-ml filtered seawater, and mixed with 5 μl of a 1.0 mg/ml solution of Calcofluor White. After staining for 10 min, the sample was centrifuged, aspirated to a pellet, and resuspended in 2–10 ml of filtered seawater for analysis. Subsamples of up to 1 ml were examined at 100–200X on a Zeiss Axioskop (Thornwood, NY) with a 100 W mercury lamp and a Zeiss #2 filter set (excitation 365 nm, emission 420 nm) and were photographed with Zeiss MC 100 digital camera system.

Sequencing of large subunit (LSU) rDNA. To confirm the species identity of different *P. steidingerae* and *P. depressum* morphologies in culture, the D1–D6 region of the LSU rDNA was amplified by single-cell PCR and sequenced as described in detail in Gribble and Anderson (2006). Briefly, for both *Protoperidinium* species, single cells of varying morphologies were isolated from culture by micropipette. The single cells were used directly as template to amplify approximately 1,430 bp of the LSU rDNA containing the variable domains D1–D6, using the primers D1R (Scholin et al. 1994) and 28-1483R (Daugbjerg et al. 2000). Polymerase chain reaction products were cloned and sequenced. Sequences were edited using Sequencher 4.5 software (Gene Codes Corporation, Ann Arbor, MI) and aligned using ClustalX v. 1.83.1 software (Thompson et al. 1997).

Observation of *Protoperidinium* spp. in vivo. Live cells of *P. steidingerae* and *P. depressum* were observed in tissue culture flasks, isolated into 48- or 96-well tissue culture plates or onto microscope slides using a Nikon dissecting microscope (Melville, NY), Zeiss IM35 inverted microscope or a Zeiss Axiovert S100 inverted microscope. Digital photos were taken on a Zeiss Axiovert S100 microscope with a Sony Exwave HAD 3CCD color video camera, using Scion Image 1.62 software or on a Zeiss Axioplan 2 using a Zeiss Axiocam.

Clonal-cross time series of *Protoperidinium steidingerae*. Two 70-ml clonal cultures of *P. steidingerae*, both without cysts, were combined in a 300-ml tissue culture flask (BD Falcon 353133, Bedford, MA) with 24 ml of *D. brightwellii* as prey. The flask was filled to the top with sterile seawater, placed on a plankton wheel, and rotated under the culture conditions described above. Subsamples of 5 ml were preserved with 5% modified Bouin's solution (v/v, final concentration; Coats and Heinbokel 1982) at the time of inoculation, 16 h after inoculation, thereafter at 24-h intervals for 4 d, at 48-h intervals over the following 6 d, and finally after an additional 72 h, for a total of 10 samples over 14 d. After inoculation at 17:00, all sampling was done at approximately 09:00, 2 h after the start of the daily light period. To examine nuclear and flagellar morphology, samples were processed using the quantitative protargol staining (QPS) method (Montagnes and Lynn 1993). The entire volume of each sample was stained, and all of the cells in each sample were counted on a Nikon compound microscope at 250X to determine total cell concentration (cells/ml) at each time point. For each sample, 50–100 cells were further analyzed to determine life-history stage. Each cell was photographed at 400–500X, and cell length, cell width, nucleus length, and nucleus width were measured using a Zeiss Axioskop or Zeiss Axioplan2 equipped with a Zeiss AxioCam interfaced to Zeiss Axiovision software with scale calibration. The number of nucleoli, transverse and longitudinal flagella, and basal bodies were determined at 1,000 or 1,250X. For each sample, the percent of cells of each life-history stage was multiplied by total number of cells/ml to estimate the concentration of cells in each stage. Life-history stages in self-crosses were not quantified.

Planozygote isolations and observations of *Protoperidinium steidingerae*. To observe encystment directly and to confirm the morphological identity of planozygotes, 60 presumptive planozygotes from non-clonal cultures were isolated into 96-well plates over three different dates. Thirty-five of the cells were deposited into separate wells of a 96-well plate, with each well filled to the top with sterile sea water and *D. brightwellii*. A 25-mm glass coverslip was sealed to the top of the well using silicone grease, forming a chamber with no airspace for each isolated cell. The entire 96-well plate was rotated at 1–2 rpm on a plankton wheel. The remaining 25 cells were held in sterile seawater in separate wells of a 96-well plate without prey or rotation. All putative planozygotes were kept at 15 °C under low light on a 14 h:10 h light: dark cycle.

Cyst germination of *Protoperidinium steidingerae*. To investigate the length of the mandatory dormancy period of hypnozygotes, the time to germination was measured for cysts of known age held at a range of temperatures. A 70-ml tissue culture flask of non-clonal *P. steidingerae* culture stood without rotation for approximately 6 h to allow cysts to settle to the bottom. A pipette was used to pull 50 ml of culture from the top of the flask, leaving the cysts behind. The cyst-free culture was added to a 250-ml tissue culture flask with 15 ml each of *D. brightwellii* and *C. affinis*. The flask was filled to the top with sterile seawater and rotated under the culture conditions described above.

The flask was inspected daily on a dissecting microscope for the appearance of cysts. The first cysts were observed 5 d after inoculation. Eight days after inoculation, cysts were allowed to settle and were collected from the bottom of the flask. Individual cysts were isolated by micropipette, washed 4X in sterile seawater, and deposited into separate wells of 96-well plates, each well with 190 μl of sterile seawater. One plate containing 34 isolated cysts was placed at 15 °C, and another plate containing 36 isolated cysts was placed at 20 °C. All cysts were under low light on a 14 h:10 h light:dark cycle. One month later, the experiment was repeated, with 35 isolated cysts at each of two temperatures, 15 °C and 5 °C. All cysts were examined twice weekly until germination was first noted and every 2 d thereafter. Observations continued until no new cysts had germinated for more than 2 wk for plates at 15 °C and 20 °C and for 1 yr for cysts held at 5 °C.

Planomeiocyte morphology of *Protoperidinium steidingerae*. To examine planomeiocyte morphology and division, cysts formed in a clonal culture of *P. steidingerae* (MV0923-PO-Clone 6) over a 1-month period were collected and stored at 2 °C to

prevent germination. Nine weeks later, after the mandatory dormancy was expected to be nearing completion based on previous germination experiments, 136 individual cysts were isolated by micropipette into 96-well plates, as described above. Cysts were checked for germination several times per day. Excysted planomeiocytes were either preserved immediately (<2 h post-germination) or isolated into new 96-well plates to monitor growth and division. Because *P. steidingerae* planomeiocytes had previously been found to require rotation and feeding for survival, each isolated cell was rotated in a 96-well plate chamber containing sterile seawater and *D. brightwellii* as described above. Planomeiocytes were checked for feeding and division several times per day, and selected individuals were preserved with modified Bouin's solution and processed by QPS for examination of nuclear and flagellar morphology. The cytology of planomeiocytes was thus examined at various times post-germination: <2 h (18 cells), 9–18 h (12 cells), 48–72 h (4 cells), at the two cell stage after the first division (24 cells), and at the four cell stage after the second division (10 cells).

Cytology of life-cycle stages of *Protoperidinium depressum*. Eight replicate 70-ml tissue culture flasks (Falcon, 35009, Becton Dickinson (BD) Biosciences) were each inoculated with 5 ml of *P. depressum* clonal culture, 3 ml of *D. brightwellii* culture, 3 ml of *C. affinis* culture, and 1 ml of *L. polyedrum* culture, filled with filtered seawater, and cultured as described above. Fourteen days later, the contents of all flasks were combined and 10.5 ml of culture was redistributed into each of 10 new 35-ml tissue culture flasks (BD Biosciences 353107), along with 3 ml of *D. brightwellii*, 3 ml of *C. affinis*, and 1 ml of *L. polyedrum*. Flasks were maintained under the culture conditions described above. Beginning immediately after inoculation, a single flask was harvested at each of nine time points at intervals of 1–4 h over a 21-h period. From each flask, 19 ml was preserved with 5% modified Bouin's solution (v/v, final concentration) and stored at room temperature. Select samples from the time series and six additional Bouin's preserved samples taken randomly from a batch culture of *P. depressum* were processed by QPS and examined as above.

RESULTS

In vivo and SEM observations for batch cultures of *Protoperidinium steidingerae*. Examination of living cells and thecal plate morphology using SEM and Calcofluor staining confirmed identity of the species under study as *P. steidingerae* Balech. In culture, *P. steidingerae* exhibited a variety of cell morphotypes, including large biflagellate cells (>78 μm), small biflagellate cells (<68 μm), large tri-flagellate cells (>90 μm), and cysts. Large biflagellate cells had a single transverse and single longitudinal flagellum, dark pink pigmentation to the cytoplasm, long, sharply tapering apical and antapical horns, and a displaced cingulum with sulcal lists (Fig. 1, 2). These large biflagellate cells swam, fed on diatom prey, and divided, but were never seen to fuse together. Given the flagellar number, behavior, and reproductive pattern, this morphotype was classified as a vegetative cell. Vegetative cells showed a four-sided apical plate occupying the position of the 1′ plate, but separated from the apex of the cell by a long suture, so that the plates homologous to the 2′ and 4′ plates were adjacent on the ventral side of the cell (Fig. 2). A single, six-sided intercalary plate was present on the dorsal side of the cell, posterior to a small dorsal 3′ plate (Fig. 3).

Before division, vegetative cells became immotile and the cytoplasm contracted from the horns and sides of the theca, forming a predivision cyst inside the theca of the parent cell. Flagella were not visible in the division cysts before cytokinesis and were presumably lost, resorbed, or stopped beating as the parent cell lost motility. Cytokinesis began with invagination of the cytoplasm, visible at two opposite points along the edge of the cell. Within 10–30 min after becoming immotile, the cell divided obliquely across the longitudinal axis of the parent theca, forming two lobes (Fig. 10). The cinguli of the daughter cells became apparent as grooves in the two lobes.

As the daughter cells began to move, the parental theca appeared to dissolve until only a membrane-like structure surrounded the daughter cells. The daughter cells that emerged from the parental membrane-like enclosure were one-third to one-half the size of the parent cell, had pink pigmentation like the parent cell, were weakly thecate or athecate, and were relatively amorphous, lacking the pronounced apical and antapical horns and sulcal or cingular lists of vegetative cells (Fig. 11). The cells were attached with the apical horn of the posterior daughter cell connected to the sulcal region of the anterior daughter cell, though the two cells were able to spin and articulate relative to one another. Within 10–20 min, daughter cells increased in size and expanded their apical and antapical horns, growing to a size near that of typical vegetative cells (Fig. 12, 13). Daughter cells separated at varying stages of development, either while still rounded or after nearly fully-developed vegetative morphology was attained.

Division of smaller than average vegetative-type cells, particularly in older cultures, resulted in very small daughter cells presumed to be gametes (Fig. 14). These divisions followed the same pattern as that for division of vegetative cells. Presumptive gametes had thick thecal plates, clear to pale-pink cytoplasm, shallowly excavated cingulum and sulcus, a sharply pointed apical horn, and two shorter, pointed, hollow antapical horns. They were easily distinguished from recently divided daughter cells by their size, heavier thecae, and lack of rounded horns. Gametes were never observed to feed. Swarming gametes collected at the bottoms of culture flasks, although mating within these swarms was not observed. Paired and fusing gametes were commonly encountered in cultures. Fusing gametes were isogamous and moved vigorously, wriggling and spinning in circles, but did not swim directionally. Plasmogamy occurred as the cells merged at a 90° angle with two longitudinal flagella and one or two transverse flagella apparent (Fig. 15).

Putative planozygotes could be distinguished by their two longitudinal flagella and single transverse flagellum (Fig. 16). The apical and antapical horns of planozygotes often appeared to be longer and thinner than those of vegetative cells. The cytoplasm of planozygotes was less darkly pigmented than in vegetative cells. Some planozygotes were smaller than average, had relatively clear pigmentation, and had shorter antapical horns that were bent or splayed distally (Fig. 17). Given their small size and ''lumpy'' appearance, we hypothesized that these were early stage planozygotes, the result of recent gamete fusion.

Cysts presumed to be hypnozygotes were encountered frequently in older cultures. These were immotile, darkly pigmented cells that settled to the bottom of the culture flask and sometimes remained in the thecae of the cells from which they originated (Fig. 4). Putative hypnozygotes were smooth-walled and dorsoventrally compressed, but varied in gross morphology, with apical and antapical horns that ranged from long and narrow to short and rounded. The cytoplasm ranged in color from grey to brown and was surrounded by a thick wall. Pink granular material was often apparent inside the cells. The outline of an intercalary archeopyle was clearly evident in SEM (Fig. 5).

Sexual processes were homothallic, with all sexual stages and dormant cysts forming in clonal cultures. While gametes were usually present in high proportions in clonal cultures, there were often relatively few hypnozygotes in these cultures. Casual observations of cultures indicated that non-clonal cultures and out-crosses usually resulted in greater production of dormant

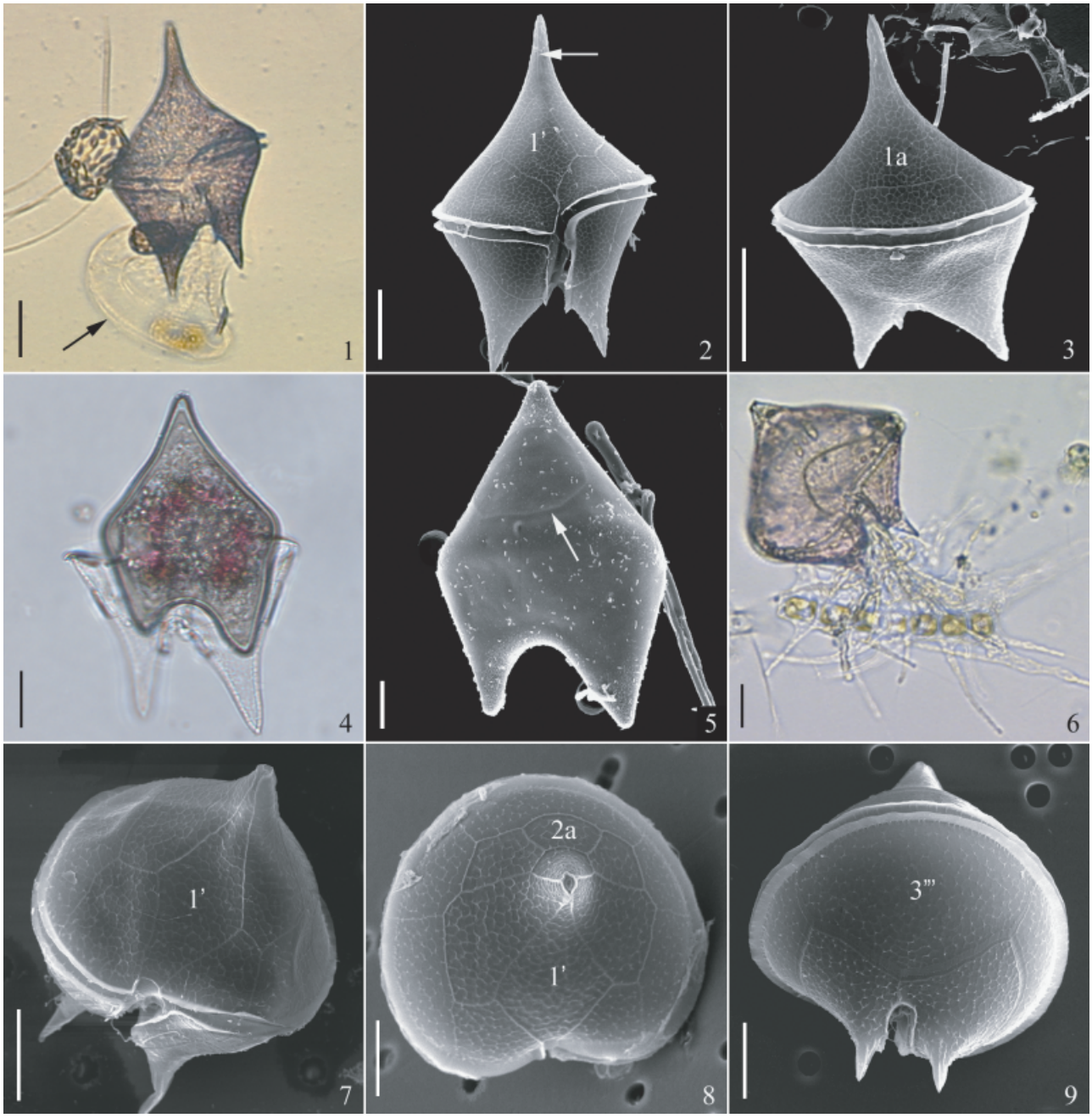

Fig. **1–9.** *Protoperidinium steidingerae* and *Protoperidinium depressum* viewed in vivo and by scanning electron microscopy (SEM). **1.** Ventral view of *P. steidingerae* in vivo with feeding veil (arrow) deployed to consume *Ditylum brightwellii*. **2.** Ventral side of *P. steidingerae* in SEM with arrow at suture separating 1′ plate from apex. **3.** Dorsal view of *P. steidingerae* showing the single intercalary plate (1a). **4.** Live hypnozygote of *P. steidingerae* inside posterior half of planozygote theca. **5.** Scanning electron micrograph of *P. steidingerae* hypnozygote with arrow at six-sided intercalary archeopyle. **6.** Ventral view of *P. depressum* in vivo consuming *Chaetoceros* sp. cells. **7.** Scanning electron micrograph of *P. depressum* showing ventral epitheca with four-sided 1′ plate. **8.** Scanning electron micrograph of *P. depressum* epitheca showing four-sided 1′ plate and three intercalary plates, including four-sided 2a plate. **9.** Dorsal hypotheca of *P. depressum* in SEM, showing large 3′′′ plate and two antapical plates. Scale bars = 20 μm.

hypnozygotes. Despite isolation and observation of 60 putative planozygotes, hypnozygote formation was not witnessed. No feeding or division was observed in any isolated planozygotes. Whether the isolated planozygotes were rotated or stationary, all died within 2–3 days.

Clonal-cross time series for *Protoperidinium steidingerae*. A cross of two clonal cultures of *P. steidingerae* was sampled over 2 wk in an attempt to better document the timing and development of life-history stages leading to encystment (Fig. 18). The abundance of *P. steidingerae* at the initiation of the experiment was 24 cells/ml, partitioned as large biflagellate cells (presumed vegetative cells) at 12 ml^{-1} (50% of the population), small biflagellate cells (gametes as described above) at 10 ml^{-1} (42%), dividing cells (presumed mitotic division) at 1 ml^{-1} (5%), and large and small cells of uncertain identity at 0.5 ml^{-1} each. Total cell abundances dropped 41% to 14 cells/ml over the first 16 h

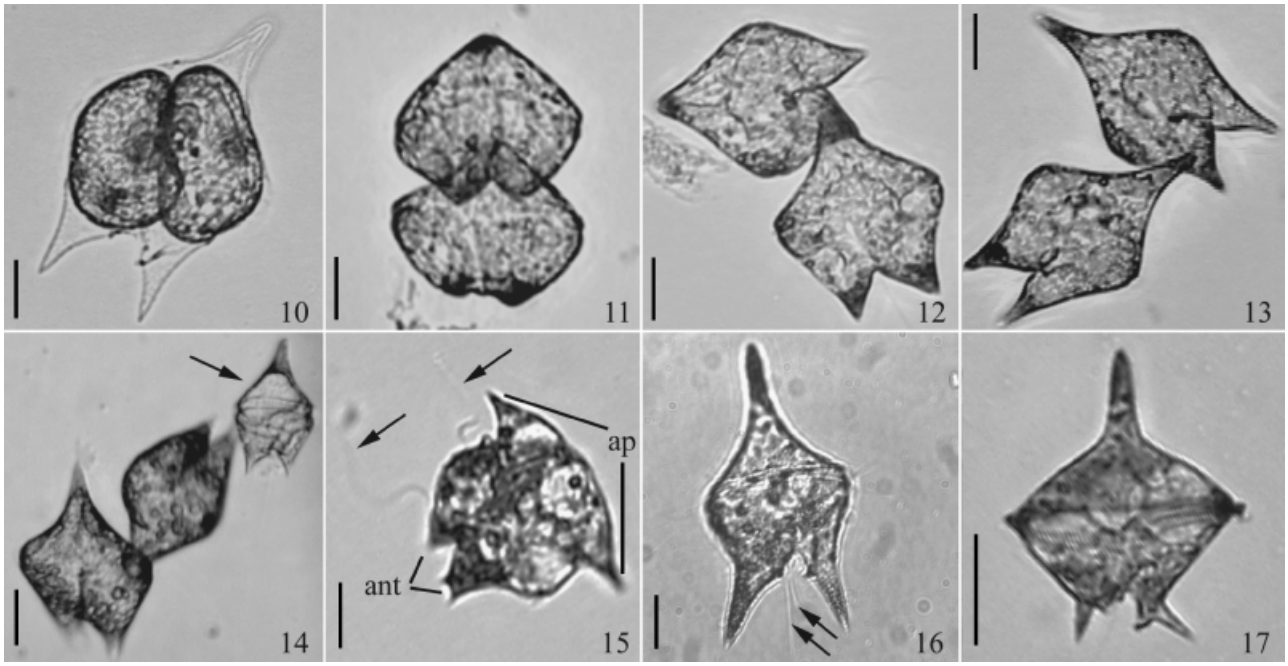

Fig. **10–17.** Dividing cells, gametes, and planozygotes of *Protoperidinium steidingerae* in vivo. **10–13.** Sequential images during division of a vegetative cell. **10.** Oblique cytokinesis inside parental theca (eleutheroschisis). **11.** Newly emerged daughter cells with undeveloped apical and antapical horns. **12.** Daughter cells attached epitheca to hypotheca and increased in size. **13.** Daughter cells with nearly fully formed apical and antapical horns. **14.** Daughter cells not yet separated, adjacent to a gamete (arrow). Note difference in size, shape, development of theca, and density of cytoplasm between recently divided cells and gamete. **15.** Paired gametes undergoing plasmogamy. Apical horns (ap), antapical horns (ant), and longitudinal flagella (arrows) are visible. **16.** Planozygote showing two longitudinal flagella (arrows). **17.** Small planozygote with narrow apical horn and distally splayed antapical horns. Scale bars = 20 μm.

after the clonal cultures were mixed. *Protoperidinium steidingerae* showed exponential growth over the next 144 h, reaching a peak density of 124 cells/ml at 160 h before the population began to decline.

The abundance of putative vegetative cells rose considerably through the first half of the time series, reaching a peak of 30 cells/ml (24%) at 160 h (Fig. 18). The concentration of vegetative cells subsequently declined to 1 cell/ml at 208 h, before increasing slightly to 6 cells/ml at the end of the experiment (328 h). Protargol-stained vegetative cells averaged 103 ± 10 μm long by 67 ± 9 μm wide (Table 1) and had a single pair of basal bodies in the sulcal region associated with a single longitudinal flagellum and a single transverse flagellum (Fig. 19). The nucleus was oval, averaged 26 ± 4 μm wide and 17 ± 2 μm long, and contained one or two round to oval nucleoli (Fig. 19, inset).

The concentration of dividing cells increased sharply through the first 88 h, concurrent with the increase in the concentration of vegetative cells (Fig. 18). During that period, the number of dividing cells changed from 1 cell/ml (5% of the population) to 12 cells/ml (40% of the population), then gradually declined to 1 cell/ml (12% of the population) over the next 170 h. From protargol-stained specimens of similar size, shape, and number of flagella as vegetative cells, but with different nuclear morphologies, a likely series of stages leading to division was inferred. In the early stages of division, the nucleus lengthened to an elongate oval that averaged 36 μm wide, had a width:length of 2.1 (Table 1), and was oriented obliquely relative to the longitudinal axis of the cell (Fig. 20). In later stages preceding cytokinesis, the chromosomes within the nucleus formed long, darkly staining strands oriented generally parallel to one another in an anterior–posterior direction, and the nucleolus or nucleoli stretched and became irregularly shaped. As division progressed, the nucleus became nearly rectangular, and the chromosomes appeared to be separating in an apical-antapical orientation along the center of the nucleus (Fig. 21). The nucleolus or nucleoli were often difficult to see at this stage, as the entire nucleus stained very darkly. These specimens had a single longitudinal flagellum and a single transverse flagellum. Two pairs of basal bodies were visible, indicating that the basal bodies had replicated prior to cytokinesis. The nuclei of the two daughter cells were fully separated as cytokinesis was completed (Fig. 22). Within the division cyst, daughter cells each had a single pair of basal bodies located near the adjacent edges of the cells. Newly formed flagella were usually associated with each cell, although it was difficult to distinguish the transverse from the longitudinal flagellum. Protargol-stained daughter cells of *P. steidingerae* were, on average, one-third to one-half the size of typical vegetative cells, averaging 55 ± 13 μm long by 42 ± 6 μm wide (Table 1). Young vegetative daughter cells had a relatively smaller length:width ratio than gametes.

The abundance of putative gametes remained low (<7 cells/ml) from 16 h through 88 h then increased dramatically to 74 cell/ml (Fig. 18). The rise in the number of gametes lagged behind the peak in cell division at 72 h and coincided with the maximum abundance of vegetative cells. Gametes ranged in size from 25 to 68 μm and had a single trailing flagellum, a single transverse flagellum, and one pair of basal bodies (Fig. 23). Gamete nuclei were round to oval in shape, averaged 13 ± 2 μm wide and 10 ± 1 μm long and contained one or two round nucleoli (Table 1; Fig. 57).

Fusing gametes were rarely encountered during the time-series and showed no discernable pattern relative to the occurrence of planozygotes (Fig. 18). A series of events in the formation of planozygotes was inferred from protargol preparations of samples from the clonal-cross time series and from batch cultures. As noted in living cells, paired gametes were connected by a

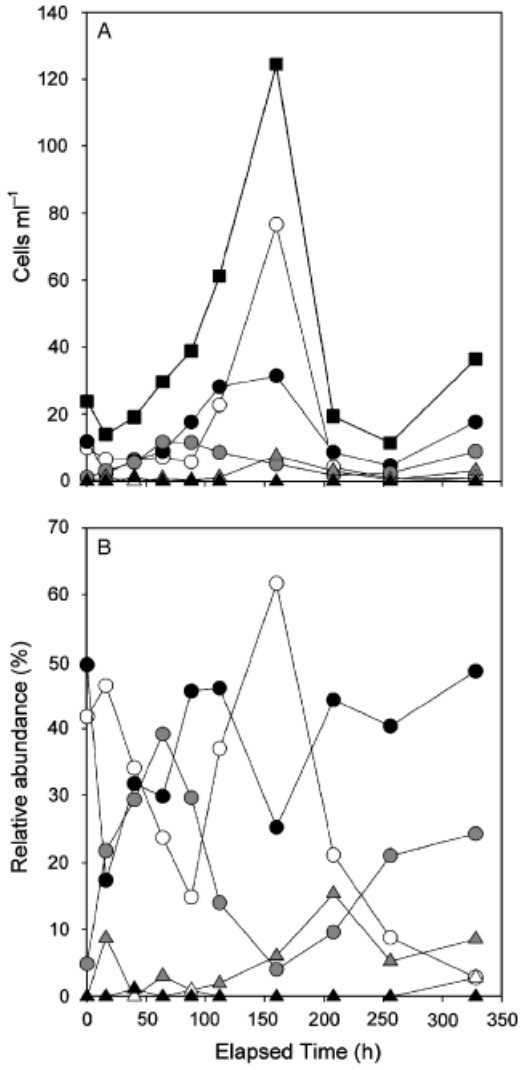

Fig. **18.** Results of clonal-cross time-series sampling of *Protoperidinium steidingerae* culture that began with vegetative cells and gametes. (**A**) Concentrations of various life-cycle stages at each sampling time in cells/ml. (**B**) Relative abundances of various life-cycle stages at each sampling time in percent. Total cells (black square), vegetative cells (black circle), dividing cells (grey circle), gametes (white circle), fusing gametes (black triangle), planozygotes (grey triangle), cysts (white triangle).

conjugation globule (sensu von Stosch 1973) that joined cells mid-ventrally in the region of the basal bodies of ventrally opposed cells aligned in a parallel to oblique, apical-to-antapical orientation (Fig. 24, 25). Karyogamy did not accompany plasmogamy (Fig. 26), resulting in early stage planozygotes with two distinct nuclei (Fig. 27). During karyogamy, the nucleus formed two lobes (Fig. 28), before coalescing into a single, oval-shaped nucleus (Fig. 29). The nucleoli remained separate at least initially, but appeared to fuse eventually, as ''fully formed'' planozygotes had as few as one nucleolus.

Putative planozygotes (tri-flagellated cells) were not detected at the initiation of the clonal-cross time-series experiment, but appeared 16 h after the two cultures were mixed (Fig. 18). Planozygotes were in low abundance from 16 to 160 h at which time their concentration increased by 5x to 7 cells/ml (6% of the population), simultaneous to the peak in presumptive gametes. Protargol-stained planozygotes had two pairs of basal bodies lying together at the base of the sulcus (Fig. 28, inset), two fully developed longitudinal flagella (Fig. 29), one transverse flagellum, and a large oval nucleus averaging 24 ± 6 μm wide by 15 ± 3 μm long (Table 1). Nucleoli ranged in number from 1 to 4, averaging more than two per cell. Planozygotes were smaller than vegetative cells, averaging 98 ± 18 μm long by 55 ± 12 μm wide, but the cell length:width ratio was not different than that of vegetative cells (Table 1).

Cysts (presumed hypnozygotes) first appeared at 88 h, 72 h after the appearance of the first planozygote (Fig. 18). They were not abundant, were often undetectable through the remainder of the experiment, and never exceeded 1 cell/ml. Hypnozygotes averaged 83 ± 7 μm long by 59 ± 5 μm wide, but ranged in size from 68 to 95 μm long by 48–68 μm wide (Table 1). All but a few were resistant to protargol staining. Hypnozygotes had an oval, darkly-staining nucleus (Fig. 30) that was noticeably smaller than that of vegetative cells. The nucleus averaged 18 ± 5 μm wide by14 ± 3 μm long and contained two or three nucleoli (Table 1). Hypnozygotes had two pairs of basal bodies (Fig. 30, inset), but apparently lacked flagella.

Cyst germination and planomeiocyte morphology for *Protoperidinium steidingerae*. Hypnozygotes of *P. steidingerae* germinated 67–74 d after their formation, indicating a mandatory dormancy period of approximately 10 wk. The temperature of incubation influenced the time to germination of the hypnozygotes (Fig. 36). At 15 °C, cysts germinated after an average of 74.6 ± 10.6 and 71.6 ± 10.1 d in the two trials. Cysts incubated at 20 °C matured only slightly more quickly, averaging 67.9 ± 9.7 d. Cysts incubated at 5 °C, however, did not germinate even after 1 yr. Maximum germination was approximately 80% at 20 °C. Although the rates of germination were similar in two separate tests of germination at 15 °C, maximum germination only reached 57% in the second trial compared with 83% in the first trial.

Germination of hypnozygotes was frequently witnessed during the cyst mandatory dormancy and the planomeiocyte morphology experiments. The empty wall of germinated hypnozygotes had an intercalary archeopyle with an attached operculum (Fig. 31). The opening was six-sided, but in some specimens appeared to be a curving slit, as the operculum usually remained slightly covering the archeopyle. Upon excystment one or both antapical horns sometimes became stuck in the cell wall (Fig. 32) either leading to the death of the cell or resulting in a planomeiocyte with one long antapical horn and one shorter, stubby horn. The gross morphology of planomeiocytes was otherwise similar to that of vegetative cells. Planomeiocytes ranged in size from 93 to 129 μm long by 53–64 μm wide in protargol stains with a cell length:width ratio of 1.9, slightly higher than that of any other stage (Table 1). They had two longitudinal flagella (Fig. 33, 34) and one transverse flagellum. Two pairs of basal bodies were present, but often were not as readily visible as in planozygotes.

As in the hypnozygotes, the nuclei of protargol-stained planomeiocytes were compact and round (Fig. 34), averaging 16 ± 2 μm in diameter (Table 1), with one or two nucleoli. In a single protargol-stained specimen sampled approximately 72 h post-germination, the nucleus was 39 μm wide by 11 μm long, stretching across the entire width of the cell (Fig. 35). The contents of the nucleus were grainy, rather than darkly staining and filamentous as in a dividing cell. The single nucleolus was large and centered in the nucleus.

Living planomeiocytes were often observed to feed before division. Planomeiocytes that were not rotated did not feed or divide, and died within several days of germination. The first division occurred 3–7 d after germination, averaging just over 4 days. Division of planomeiocytes was by eleutheroschisis, and in

Table **1.** Cell size, nucleus size, and number of nucleoli in various life-history stages of *Protoperidinium steidingerae*.

		Vegetative	Early division	Late division	Daughter cells	Gametes	Planozygotes	Hypnozygotes	Planomeiocytes
Cell length (μm)	Mean	103.6	108.9	107.3	55.3	48.1	97.9	82.5[b]	111.6
	S	9.7	11.5	10.5	12.7	6.5	17.9	7.3	9.4
	Range	77.6–125.0	81.5–135.0	95.0–127.5	37.0–73.3	24.9–67.8	55.0–140.0	67.5–95.0	93–129
Cell width (μm)	Mean	63.2	66.9	66.8	42.3	34.1	55.4	58.8[b]	58.7
	S	6.7	8.7	6.5	5.9	4.5	12.3	5.1	3.3
	Range	45.3–82.0	30.7–82.8	55.0–79.0	33.5–50.6	24.0–44.5	29.2–74.2	47.5–67.5	53.4–63.6
Cell length:width	Mean	1.7	1.6	1.6	1.2	1.4	1.7	1.4[b]	1.9
	S	0.1	0.1	0.1	0.2	0.2	0.1	0.1	0.2
	Range	1.3–2.2	1.4–1.9	1.4–1.8	0.9–1.6	0.6–1.8	1.5–1.9	1.2–1.8	1.6–2.2
Nucleus width (μm)	Mean	25.9	34.5	35.9	18.0	13.3	23.9	18.1[a]	15.6
	S	3.8	6.4	5.1	4.9	2.4	5.5	5.0	2.2
	Range	12.0–38.0	10.5–45.0	28.5–49.3	11.0–25.5	8.0–20.4	10.5–33.7	12.6–25.2	11.5–19.5
Nucleus length (μm)	Mean	16.2	16.9	17.5	12.5	9.9	14.8	13.9[a]	15.6
	S	2.5	3.0	4.0	3.4	1.4	2.7	3.2	2.1
	Range	9.1–23.0	10.5–25.5	12.5–27.0	8.0–18.5	6.3–18.3	9.7–19.0	8.2–16.6	11.7–20.0
Nucleus width:length	Mean	1.6	2.1	2.1	1.4	1.4	1.6	1.4[a]	1.0
	S	0.2	0.3	0.5	0.2	0.3	0.3	0.5	0.2
	Range	1.2–2.8	1.0–2.9	1.2–2.8	1.1–1.8	0.7–2.6	1.0–2.5	0.9–2.1	0.7–1.6
Number nucleoli	Mean	1.2	1.3	1.7	1.3	1.5	2.2	2.3[a]	1.2
	S	0.4	0.4	0.7	0.5	0.5	0.9	0.5	0.4
	Range	1.0–2.0	1.0–2.0	1.0–3.0	1.0–2.0	1.0–2.0	1.0–4.0	2.0–3.0	1.0–2.0
n		187	87	26	19	133	26	30[b]	18

Data were from protargol-stained specimens from a clonal-cross time-series experiment, unless otherwise noted. Number of cells measured for each stage indicated by ''*n*.'' Standard deviation indicated by ''*S*.''

[a]From seven cells in both time series.

[b]From protargol-preserved cysts formed in culture of strain MV0802-2.

live planomeiocytes was indistinguishable from division of vegetative cells. The size and shape of daughter cells was like that of daughter cells from vegetative division. The nuclei of daughter cells from planomeiocyte division were larger and more elongate than those of the planomeiocytes, with an average width of 21.3 ± 2.5 μm and an average length of 16.8 ± 2.2 μm. The average width:length ratio of the nucleus was 1.3, halfway between that of planomeiocytes (1.0) and vegetative cells (1.6). The nucleolus was usually shifted to one side of the nucleus in planomeiocyte daughter cells. The second planomeiocyte division occurred within 1–2 d of the first division, and the resulting cells had the same morphology as vegetative cells.

In vivo and SEM observations for batch cultures of *Protoperidinium depressum*. Examination of living cells and thecal plate morphology using SEM and Calcofluor staining confirmed the identity of the species under study as *P. depressum* (Bailey) Balech and revealed differences in thecal plate morphology between presumptive vegetative cells and gametes. Vegetative cells were large, measuring 90–110 μm long by 80–120 μm wide in vivo, had dark pink pigmentation (Fig. 6), a single longitudinal flagellum, and a single transverse flagellum. The epitheca of vegetative cells was convex near the cingulum, then steeply sloped and became nearly concave approaching the apical horn. The cingulum had lists supported by spines. The large 1′ plate was four-sided (Fig. 7, 8). There were three dorsal intercalary plates, with a four-sided 2a plate (Fig. 8). Two antapical plates covered the short antapical horns (Fig. 9). Vegetative cells swam, fed on diatoms, and divided to form daughter cells, but were never observed to form pairs or fuse together. Binary fission of vegetative cells took place inside an immotile division cyst. The cytoplasm contracted from the apical and antapical horns and the sides of the parental theca. (Fig. 37). In approximately 15–30 min, a division furrow formed first at the edge of the division cyst, then extended obliquely through the cytoplasm to divide the cell into two oblong

Fig. **19–35.** Protargol-stained and live *Protoperidinium steidingerae* from clonal-cross and cyst germination experiments. **19.** Vegetative cell with one trailing flagellum (black arrow), one transverse flagellum (white arrow), and oval-shaped nucleus (arrowhead). **Inset.** Close-up of nucleus of a vegetative cell; scale bar = 5 μm. **20.** Vegetative cell with elongate nucleus oriented obliquely across the cell and containing densely stained chromosomes. **21.** Higher magnification of dividing nucleus with separating chromosomes. **22.** Division cyst undergoing cytokinesis, but after completion of karyokinesis, with daughter nuclei (arrows) widely separated. **23.** Gamete with single trailing flagellum (black arrow), single transverse flagellum (white arrow), and round-oval nucleus (arrowhead). **24.** Paired gametes in early stage of fusion showing conjugation tube extending between the two cells (arrow). **25.** Higher magnification of conjugation tube in another pair of gametes. **26.** Gametes in late stage of fusion with a arrows indicating position of the two gamete nuclei. Apical and antapical horns protrude from edges of fusing cells. **27.** Planozygote following plasmogamy, but prior to karyogamy as indicated by the two separate nuclei (arrowheads). **28.** Planozygote at intermediate stage of karyogamy showing fusing gamete nuclei (black arrowheads) and two trailing flagella (arrows). **Inset.** Close-up of two pairs of basal bodies (white arrowheads) associated with the planozygote flagella; scale bar = 1 μm. **29.** Planozygote following completion of karyogamy showing two trailing flagella (arrows) and a single oval nucleus (arrowhead). **30.** Recently encysted hypnozygote with round, compact nucleus (arrow). **Inset.** Close-up of sulcal region showing two pairs of basal bodies (arrowheads); scale bar = 1 μm. **31.** Empty hypnozygote wall possessing archeopyle with attached operculum (arrow). **32.** Excysting planomeiocyte in vivo with right antapical horn (arrowhead) stuck in cyst wall. Unable to escape from the cyst, this cell later died. **33.** Live planomeiocyte with arrow indicating two longitudinal flagella. **34.** Protargol stain of recently excysted planomeiocyte with small, round nucleus (arrowhead) and two longitudinal flagella (arrows). **35.** Planomeiocyte approximately 72 h after excystment. Note extension of nucleus across the width of the cell, grainy appearance of nucleoplasm, and large, centrally located nucleolus (arrow). Scale bars = 20 μm, except as noted for insets.

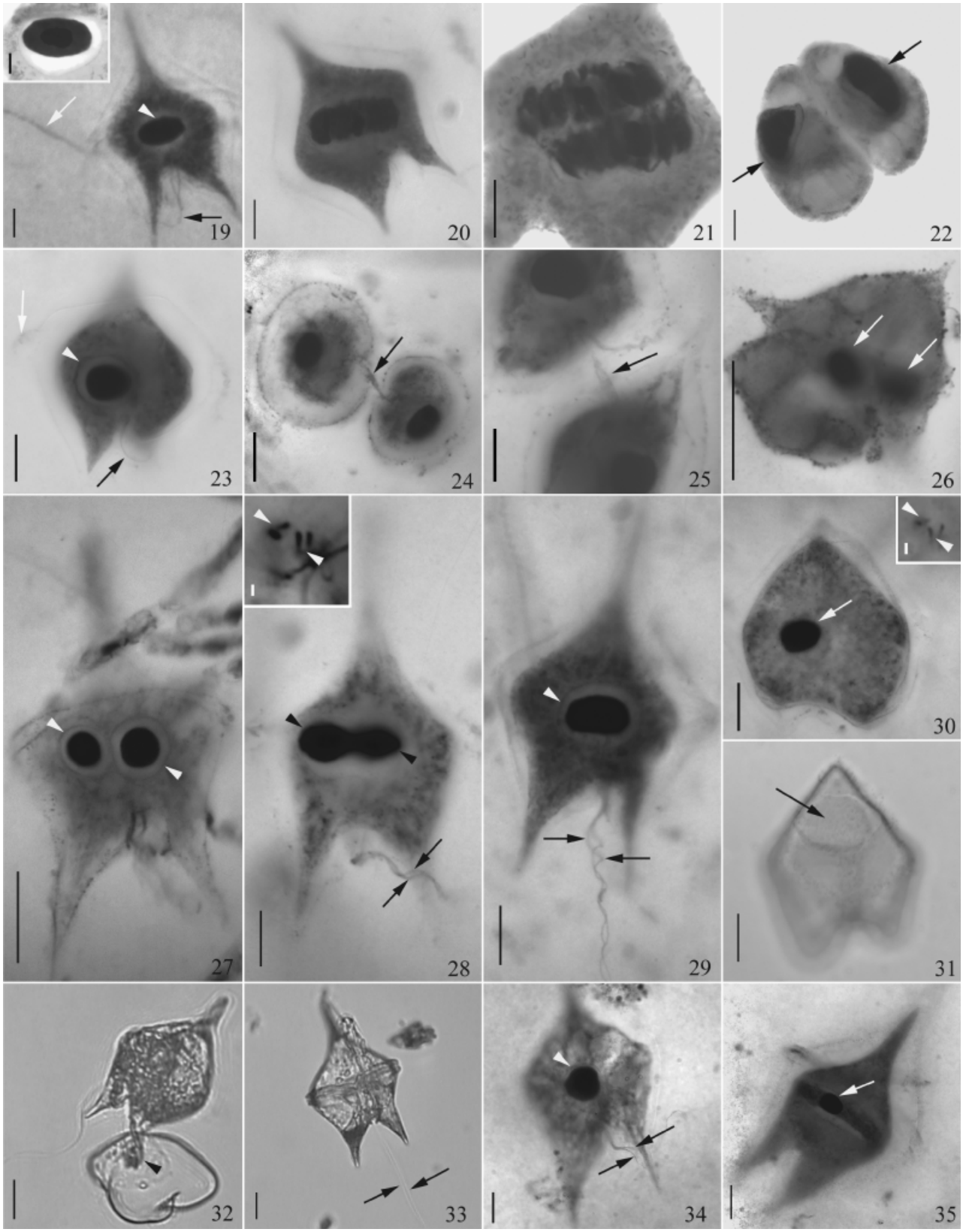
19
20
21
22
23
24
25
26
27
28
29
30
31
32
33
34
35

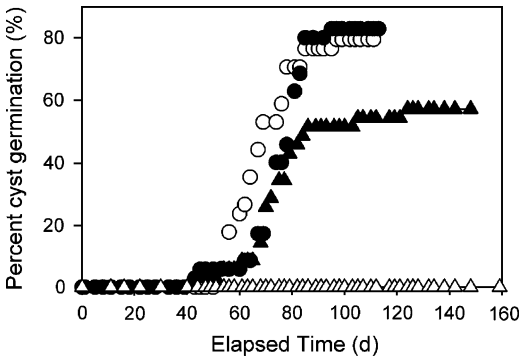

Fig. **36.** Cumulative percentage germination over time of *Protoperidinium steidingerae* hypnozygotes incubated at a range of temperatures, showing mandatory dormancy period. Two separate treatments at 15 °C are shown. 20 °C (dark circle), 15 °C treatment 1 (white circle), 15 °C treatment 2 (black triangle), 5 °C (white triangle).

lobes (Fig. 38). Within 2 h of division cyst formation, two daughter cells emerged, breaking through the parental theca at the cingulum (Fig. 39).

Daughter cells were joined with the apical horn of one cell attached in the mid-posterior sulcal region of the other cell (Fig. 40). Daughter cells were approximately half the size of the parent cell (60–90 μm long by 50–80 μm wide), weakly thecate or athecate, and relatively amorphous, lacking the pronounced apical and antapical horns of the vegetative cells and without sulcal or cingular lists. Within several minutes of division, the daughter cells increased in size and expanded their apical and antapical horns. Daughter cells remained joined for several minutes to more than 1 h before separating and developing the characteristic vegetative cell morphology of *P. depressum*.

Two successive, rapid divisions of putative vegetative cells resulting in two pairs of smaller daughter cells frequently occurred in cultures (Fig. 41–44). Division took place inside the theca of the parental cell, with the first fission producing daughter cells that were attached in an apical horn-to-sulcus configuration as described above. Daughter cells immediately entered a second division without increasing in size and sometimes before they had separated (Fig. 41). When the second division preceded separation of first generation daughter cells, four small second-generation daughter cells developed inside a delicate, membrane-like structure (Fig. 42). These separated as two pairs of cells (Fig. 43) before developing into uncoupled individuals. When first generation cells separated before the second division, they appeared to be division cysts of approximately half the size of vegetative cells (Fig. 44). The final products of the rapid two-step division remained small and became thecate with rounded apical horns and clear cytoplasm.

Small cells of similar size and morphology to those formed by the rapid two-step division were observed to pair and fuse, confirming that they were gametes. Gametes ranged in size from 50 to 60 μm long by 30–60 μm wide and had clear pigmentation, a blunt, straight-sided apical horn and two short, hollow antapical horns terminating in a sharp point (Fig. 45). The cingulum had lists supported by spines. Like vegetative cells, gametes also had a four-sided 1′ apical plate (Fig. 46), but exhibited two different dorsal epithecal morphologies. Both types had two intercalary plates rather than the three typical of *P. depressum* vegetative cells. Some gametes had a four-sided 3′ plate separated from the dorsal precingular plates by two intercalary plates, each with five sides (Fig. 47). Others had a five-sided 3′ plate that contacted the dorsal precingular plate and lay between the two intercalary plates, each of which was five-sided (Fig. 48).

Gamete fusion occurred in clonal culture, indicating that *P. depressum* may be homothallic. Fusing gametes appeared to be isogamous, with coupling occurring in either a perpendicular or parallel orientation, with their ventral-to-ventral orientation easily distinguished from the orientation of dividing cells (Fig. 49). Large cells with pink cytoplasmic pigmentation and two longitudinal flagella (presumptive planozygotes) were also present in cultures with fusing gametes (Fig. 50). Of several presumptive planozygotes isolated into wells of a 96-well plate, one exhibited nuclear cyclosis (Fig. 51). The nucleus of that individual was greatly enlarged, extending nearly across the entire width of the cell. The contents of the nucleus slowly swirled in a clockwise direction for more than 5 h from the time of initial observation. During that time, the cell was motile, although it generally remained near the bottom of the well swimming in slow clockwise circles. The cell did not divide after cyclosis ceased and died 3 days later without progressing to the next life-cycle stage. No dormant cysts or hypnozygotes were ever observed in the cultures of *P. depressum*.

Morphology of life-cycle stages of *Protoperidinium depressum* from protargol-stained specimens. Because of the strong equatorial curvature of *P. depressum* cells, most protargol-stained specimens were tilted toward the anterior or posterior making measurement of cell length unreliable. Putative vegetative cells averaged 96 ± 6 μm wide (Table 2), had one transverse and one trailing flagellum, and possessed an ovoid to spherical nucleus averaging 32 ± 3 by 24 ± 3 μm and containing one to three nucleoli (Fig. 52, 53). Basal bodies were difficult to discern due to cell orientation and heavy staining in the sulcal region, apparently associated with feeding structures. In the few cases where basal bodies could be seen, a single pair was present at the base of the flagella.

A series of events in the presumptive asexual division of vegetative cells was inferred from protargol-stained specimens. Before the formation of a division cyst, the nucleus lengthened and became reniform in shape as the nucleoli replicated (Fig. 54). Once the division cyst was formed, flagella were no longer visible, presumably having been lost or resorbed. Karyokinesis occurred simultaneously with cytokinesis, with the nucleus taking on a V-shaped configuration across the fission furrow as it separated into daughter nuclei (Fig. 55). Two basal bodies could be seen in each lobe of the division cyst after cytokinesis. Daughter cells had reniform nuclei, one to three nucleoli, a single pair of basal bodies, and a transverse and longitudinal flagellum. They were typically attached in an apical horn-to-sulcus orientation (Fig. 56).

Putative planozygotes sorted as two morphotypes differing in nuclear configuration, but sharing in common the presences of two longitudinal flagella and a single transverse flagellum. Cells of one group averaged 95 ± 5 μm wide and had round to ovoid nuclei measuring 31 ± 2 by 23 ± 2 μm and contained from three to five nucleoli (Fig. 58, 59). The nucleus of the second morphotype strongly resembled the Knäuel stage reported by von Stosch (1972). These cells were 92–108 μm wide and contained a nucleus ranging 57–71 μm in length that extended across the entire width of the cell (Table 2). The nucleoplasm was grainy due to staining of the chromosomes. A single large, round nucleolus was centered along the posterior edge of the nucleus (Fig. 60).

Molecular analysis of morphotypes of *Protoperidinium depressum* and *Protoperidinium steidingerae*. Because of the differences in the gross morphology and plate tabulation of life-cycle stages observed in *P. steidingerae* and *P. depressum* cultures, we used molecular methods to verify species identification of the different morphotypes. For each culture, single-cell PCR and sequencing of the D1–D6 region (ca. 1,430 bp) of the LSU

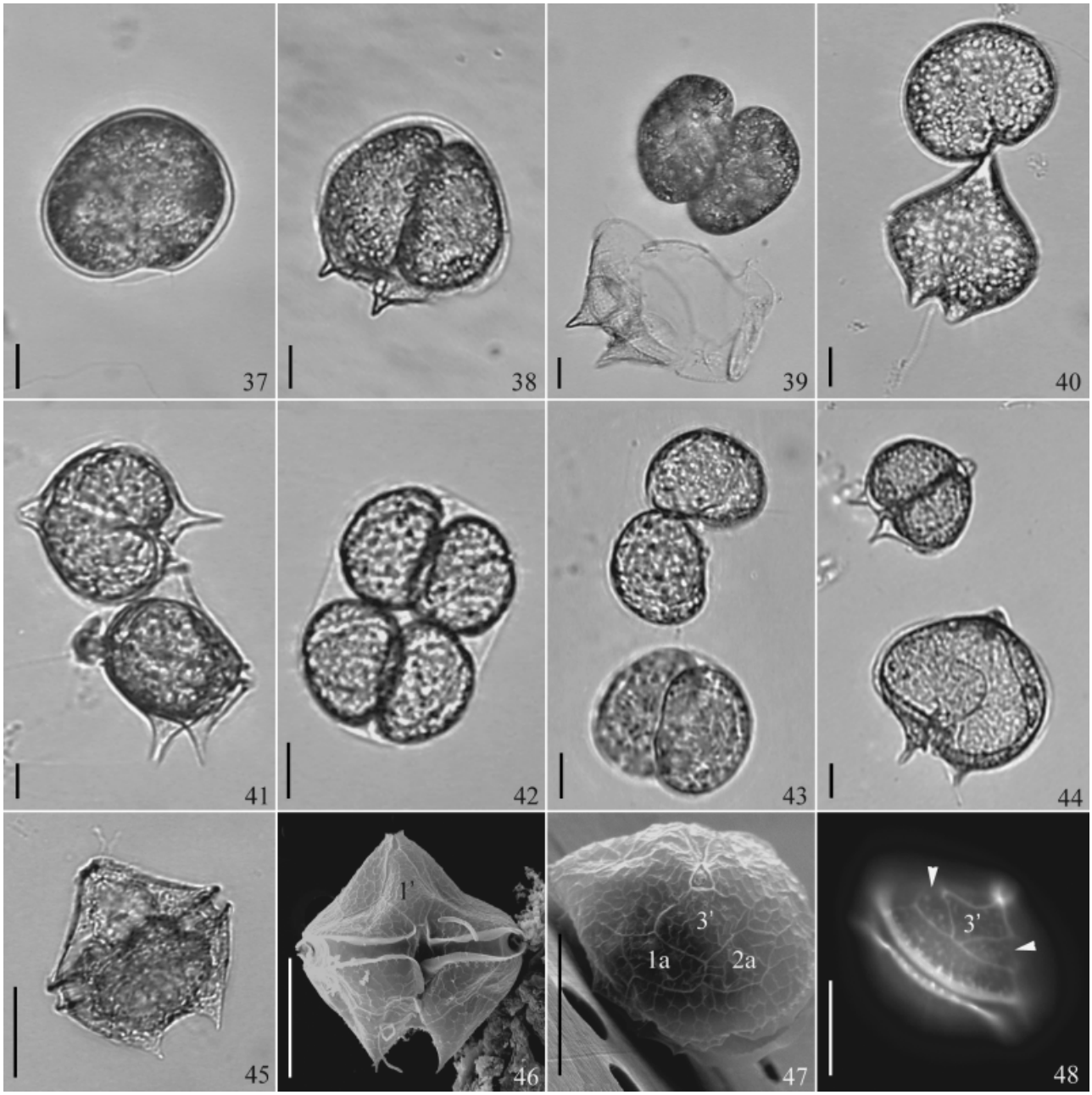

Fig. **37–48.** Dividing cells and gametes of *Protoperidinium depressum*. **37–40.** Division by eleutheroschisis to produce two daughter cells. **37.** Early division cyst before the onset of cytokinesis. **38.** Division cyst with cytoplasm of parental cell divided obliquely into two lobes. **39.** Same cell as in Fig. 38 showing attached daughter cells emerging from parental theca. **40.** Daughter cells with partially developed apical and antapical horns. **41–44.** Rapid sequential divisions to form four small daughter cells (gametes). **41.** A pair of recently divided cells that are still attached, and already undergoing a second division. Division cysts have formed and cytokinesis is occurring in each cell. **42.** Specimens shown in Fig. 41 produced a tetrad of small cells shown here surrounded by a single membrane-like structure. **43.** Tetrad from Fig. 42 emerged from the membranous enclosure as two pairs of small daughter cells without distinctive morphology. **44.** Small cell undergoing cytokinesis shown next to typical vegetative cell for comparison of size. **45.** Gamete in vivo showing rounded apical horn and short antapical horns. **46.** Scanning electron micrograph of ventral surface of *P. depressum* gamete showing four-sided 1′ plate. **47.** Scanning electron micrograph of gamete dorsal epitheca showing four-sided 3′ plate anterior to two adjacent intercalary plates (1a and 2a). **48.** Calcofluor white stained dorsal epitheca of *P. depressum* gamete, showing five-sided 3′ plate sitting between two intercalary plates (arrowheads). Scale bars = 20 μm.

rDNA of large cells with a typical vegetative morphology and of small cells with a typical gamete morphology confirmed that the morphotypes were the same species, with 100% sequence identity (data not shown).

DISCUSSION

This study described for the first time the life histories of two species of *Protoperidinium*. An array of techniques, including live

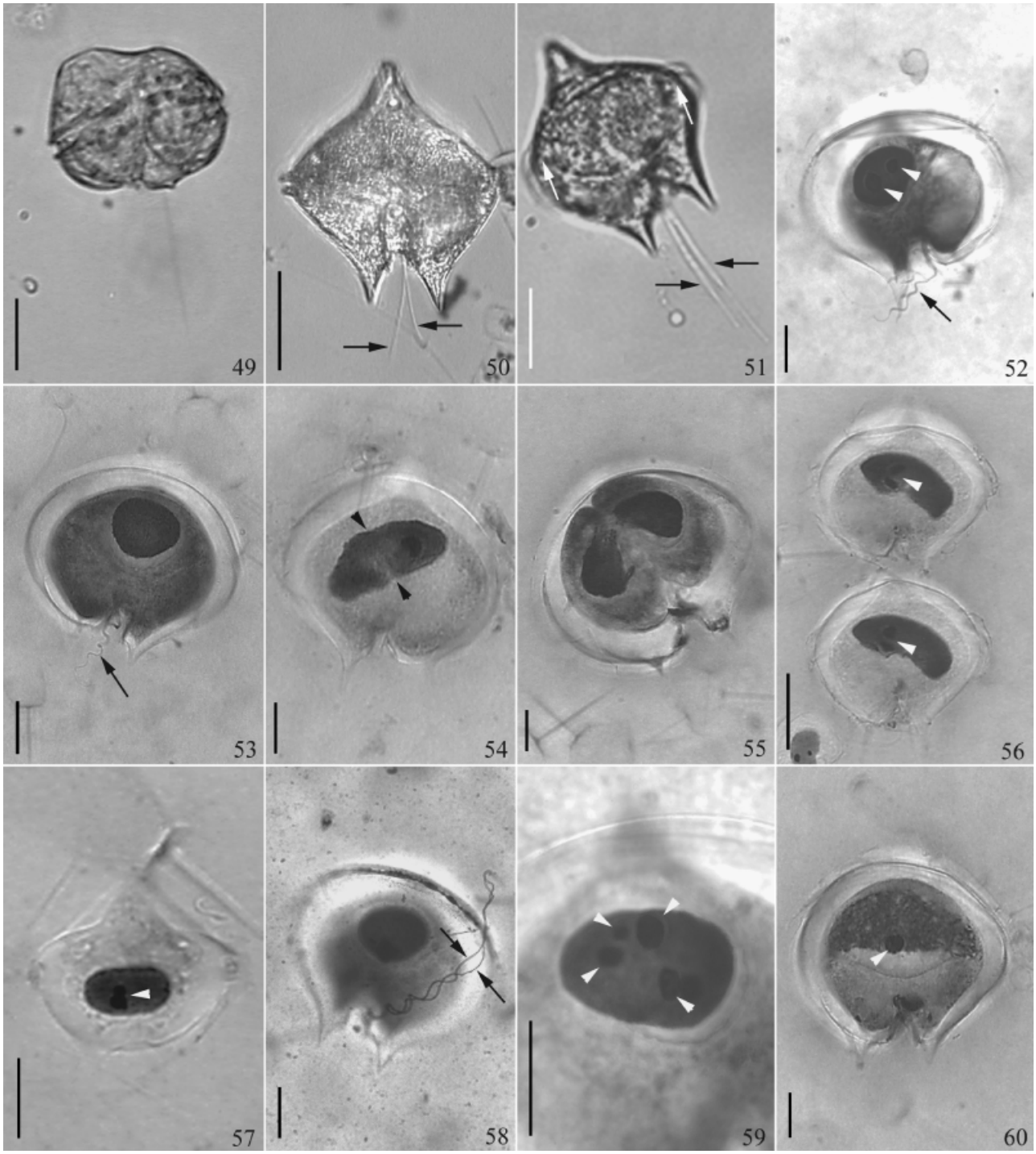

Fig. **49–60.** Live and protargol-stained *Protoperidinium depressum*. **49.** Fusing gametes oriented parallel to one another with ventral sides touching. **50.** Planozygote with two longitudinal flagella (arrows). **51.** Planozygote with enlarged nucleus (white arrows indicate lateral margins) and two longitudinal flagella (arrows). Nucleus measured nearly 80 μm across and was undergoing cyclosis. **52, 53.** Vegetative cells showing single longitudinal flagellum (arrows), compact nucleus, and two nucleoli (arrowheads). **54.** Vegetative cell undergoing karyokinesis as indicated by the elongate nucleus and equatorial constriction (arrowheads). **55.** Division cyst showing cytoplasm divided into two lobes and nucleus in telophase. **56.** Recently formed daughter cells each with two nucleoli (arrowheads). Epitheca of posterior cell is attached to sulcal region of anterior cell. **57.** Gamete with ovoid nucleus and two nucleoli (arrowhead). **58.** Planozygote with ovoid nucleus and two longitudinal flagella (arrows). **59.** Close-up of planozygote nucleus showing multiple nucleoli (arrowheads). **60.** Planozygote with enlarged nucleus, granular nucleoplasm, and single large nucleolus (arrowhead) indicative of nuclear cyclosis. Scale bars = 20 μm.

Table **2.** Cell size, nucleus size, number of nucleoli and number of flagella for different life history stages of *Protoperidinium depressum*, determined from protargol-stained specimens.

		Vegetative	Dividing	Planozygote	Nuclear cyclosis
Cell width (μm)	Mean	95.8	79.8	95.1	98.8
	S	6.0	6.0	4.8	5.9
	Range	79.2–106.6	73.1–94.5	87.7–101.5	92–108
Nucleus width (μm)	Mean	32.5	37.4	31.5	65.0
	S	3.1	3.9	1.7	5.5
	Range	26.0–37.7	29.5–43.3	23.1–34.5	57–71
Nucleus length (μm)	Mean	24.0	21.1	23.0	32.6
	S	3.1	5.8	2.3	6.3
	Range	12.1–28.7	15.8–33.5	19.0–25.8	27–40
Number nucleoli	Mean	2.0	3.3	4.1	1
	S	0.8	1.6	0.8	0
	Range	1.0–3.0	2.0–6.0	3.0–5.0	1
Number longitudinal flagella	Mean	1	1	2	2
	S	0	0	0	0
	Range	1	0–1	2	2
Number transverse flagella	Mean	1	1	1	1
	S	0	0	0	0
	Range	1	0–1	1	1
n		32	13	10	5

Standard deviation indicated by ''*S*.''

observations, time-series sampling, histological staining, morphological analysis by SEM and Calcofluor White staining, and identification by single-cell PCR and sequencing, allowed elucidation of the life history of *P. steidingerae* (Fig. 61, 62) and characterization of several life-cycle events in *P depressum*. Both species appear to have asexual and sexual cycles similar to those of other free-living dinoflagellates. Many of the life-history stages observed in *P. depressum* were similar to those observed in *P. steidingerae* Balech.

In both species, asexual division is by eleutheroschisis as defined by Pfiester and Anderson (1987), in which binary fission takes place inside the theca of the parent cell, and daughter cells form new thecae rather than share that of the parent (Fig. 61). The nucleus of a vegetative cell containing one to two nucleoli elongates and divides as basal bodies replicate. The parent cell forms a division cyst in which karyokinesis and cytokinesis occur. Daughter cells about half the size of the parent cell emerge from the parent theca without distinctive morphological features and are paired in an apical horn-to-sulcus orientation. The daughter cells increase in size before separating.

Sexual processes varied between *P. steidingerae* and *P. depressum*. In *P. depressum*, gametogenesis occurred through a two-step depauperating division, in which cells divide before synthesis of the cytoplasm is complete, resulting in four division products that were smaller and less pigmented than the vegetative cells (von Stosch 1964). This type of division was not directly observed in *P. steidingerae*, although gametes were observed in culture. Gametes of both species were isogamous and biflagellate with a single pair of basal bodies. In *P. steidingerae*, gamete fusion began with contact via a conjugation tube (Fig. 62). The planozygote resulting from gamete fusion had two pairs of basal bodies and two longitudinal flagella. The nuclei from the two gametes fused after plasmogamy to form a nucleus containing all of the nucleoli contributed by the gametes. In *P. steidingerae*, the planozygote encysted, forming a dormant hypnozygote with two pairs of basal bodies and a compact, round nucleus. The planomeiocyte excysted after a mandatory dormancy period of approximately 70 days. The planomeiocyte had two pairs of basal bodies associated with two longitudinal flagella, a single transverse flagellum, and a single, compact, round nucleus. Nuclear cyclosis occurred in the planomeiocyte, before the first division at approximately 4 days post-germination. In *P. depressum*, no hypnozygote was formed from the planomeiocyte stage. Nuclear cyclosis occurred in the planozygote stage. The fate of planomeiocytes of *P. depressum* after nuclear cyclosis was not observed.

Clonal-cross time series of *Protoperidinium steidingerae*. A probable series of events and transitions between life-history stages in asexual and sexual processes was inferred from the order of appearance of different life-history stages over time and the range of nuclear and flagellar morphologies within each stage seen in preserved samples, together with observations of live cells. In the time series, a pulse of dividing cells preceded increases in concentrations of vegetative cells and gametes. The peak in the concentrations of both vegetative cells and gametes at 160 h followed the maximum in dividing cells (16–112 h) at 88 h, suggesting that some portion of the dividing cells likely were undergoing asexual division to replicate vegetative cells, while others were differentiating to form gametes. The observation that the maximum concentration of dividing cells at 88 h was still relatively low compared with the resulting concentrations of vegetative cells and gametes at 112 and 160 h was reasonable considering that division is probably a short-lived process, so that at any one time point only a portion of the total cells undergoing division during a 24-h period was captured.

When identifying dividing cells in protargol-stained preparations, we did not distinguish between those cells undergoing typical asexual division and those undergoing gametogenesis. Dividing cells ranged in length from 81 to 135 μm; the smaller of these dividing cells may have been undergoing a depauperate division that would result in gametes. Small division cysts were observed in live cultures, and the resulting daughter cells were presumed to be gametes, based on size.

After 160 h, the concentrations of both vegetative cells and gametes declined precipitously. With 48 h between sampling points at this stage in the experiment, we may have missed additional fluctuations in concentrations after 160 h. We might speculate that most of these vegetative cells divided to form gametes, resulting in the low concentration of vegetative cells at 208 h. An increase in gamete concentration could have been missed in the time elapsed between the 160 and 208 h sampling points. Those veg-

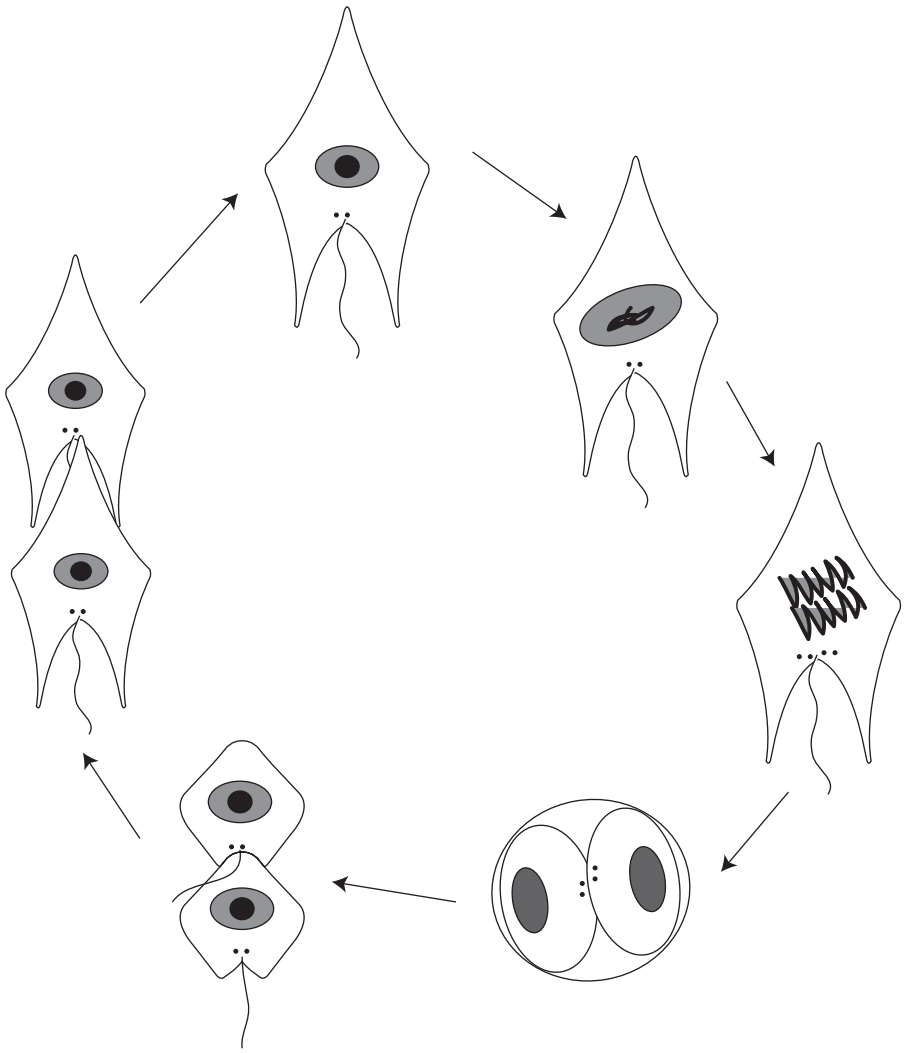

Fig. **61.** Schematic of proposed asexual cycle of *Protoperidinium steidingerae*. Nucleus of vegetative cell containing one to two nucleoli elongates and divides as basal bodies replicate. Parent cell forms division cyst, in which karyokinesis and cytokinesis occur. Daughter cells emerge from division cyst, initially small and rounded, then increasing in size before separating.

etative cells remaining after 208 h may have continued to reproduce asexually, leading to the increasing concentration of vegetative cells over the last 72 h of the experiment.

Sampling of the cross of two clonal cultures of *P. steidingerae* was conducted in the morning, and all live observations were made during daylight hours, so we may have failed to capture most gamete fusions. The large drop in the concentration of gametes and the corresponding increase in the concentration of planozygotes between the first afternoon sample and the second morning sample may indicate that gamete fusions of *P. steidingerae* occurred primarily at night. A higher occurrence of gamete fusion at night versus during the day has been previously reported for some photosynthetic dinoflagellate species (Pfiester and Anderson 1987).

Gametes preceded the appearance of tri-flagellated cells with double the number of nucleoli of vegetative cells and two pairs of basal bodies, which were classified as planozygotes. Many more gametes were produced than resulted in planozygotes in the time series. Like gametes of the heterotrophic dinoflagellate *Pfiesteria* spp. (Parrow et al. 2002), gametes of *P. steidingerae* were never observed to feed in culture. *Protoperidinium steidingerae* gametes seemed to be short lived, dying relatively quickly if they did not fuse. This hypothesis is supported by our observation that isolated gametes rarely survived more than 24 h and never more than 3 d, even if rotated.

In the clonal-cross time series, dormant hypnozygotes appeared in culture only after diploid planozygotes were detected. The similarity in the number of nucleoli, double that of vegetative cells and gametes, and the presence of two pairs of basal bodies and two longitudinal flagella indicated that the planozygotes and hypnozygotes were diploid products of sexual fusion.

While the proportion of planozygotes remained low throughout the time series, hypnozygote production by the end of the experiment was not high enough to account for encystment of all planozygotes within approximately 3 d after gamete fusion, suggesting that either not all planozygotes were viable or not all formed hypnozygotes, supported by the observation that 60 isolated putative planozygotes died without forming hypnozygotes. Alternatively, some planozygotes may persist longer than 3 d before hypnozygote formation. The reason for the low success rate of planozygote encystment is unclear. On the other hand, planozygotes may be able to divide and revert to asexual

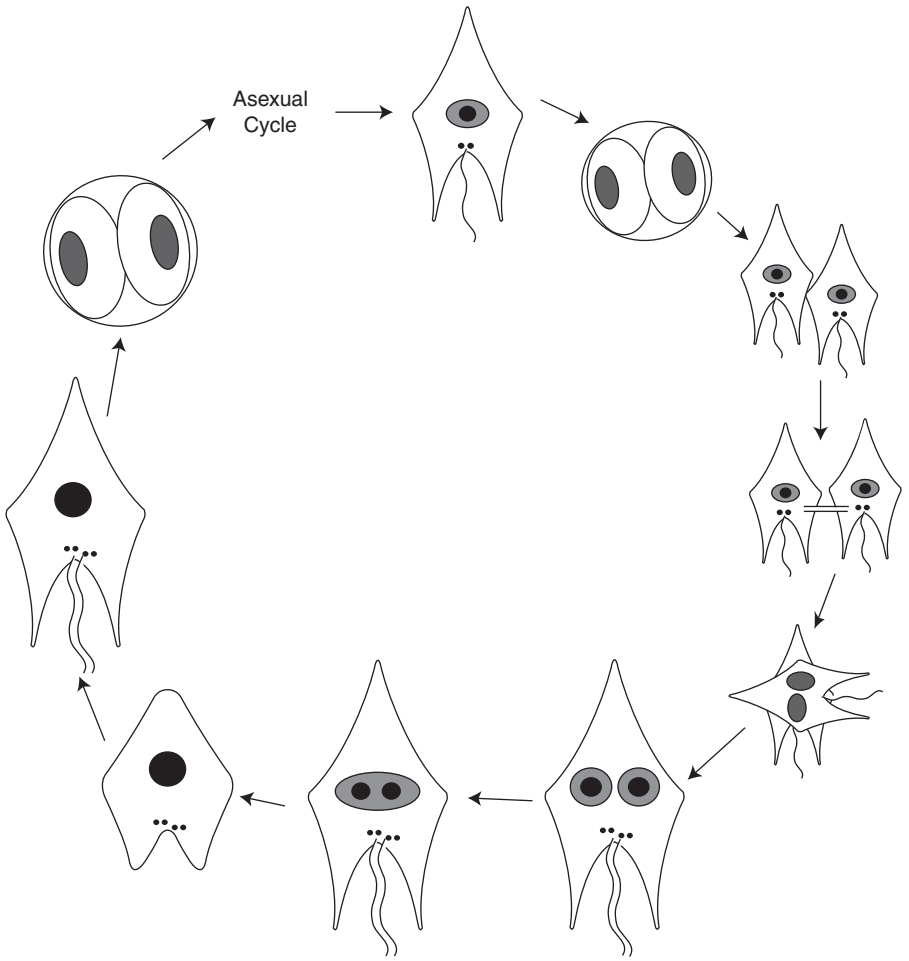

Fig. **62.** Schematic of proposed sexual cycle of *Protoperidinium steidingerae*. Gametes may form through a depauperate division. Gamete fusion begins with contact via a conjugation tube before full plasmogamy occurs. The planozygote resulting from gamete fusion has two pairs of basal bodies and two longitudinal flagella. The nuclei from the two gametes gradually fuse to form a nucleus containing all of the nucleoli contributed by the gametes. The planozygote encysts, forming dormant hypnozygotes with two pairs of basal bodies and a compact, round nucleus. The planomeiocyte excysts after a mandatory dormancy period of approximately 70 days. The planomeiocyte has two pairs of basal bodies associated with two longitudinal flagella, and a single, compact, round nucleus. The planomeiocyte divided for the first time within approximately 4 days.

reproduction without going through a hypnozygote stage, although that process was not captured by our experiments or observations. Previous studies of *Gyrodinium uncatenum* (Coats, Tyler, and Anderson 1984) and *Alexandrium tamarense* (Anderson, Kulis, and Binder 1984) have reported similar findings of many planozygotes resulting in fewer cysts than expected. Planomeiocytes were undetectable throughout the clonal-cross time series, indicating that no hypnozygotes germinated over the course of the experiment. This result corroborates the finding that hypnozygotes have a mandatory dormancy period of approximately 10 wk, far longer than the 2 wk clonal-cross time series.

Homothallism. No stressors were necessary to induce sexuality in cultures of *P. steidingerae* or *P. depressum*. Sexual processes may be constitutive, although culture artifacts like high cell density or macro- or micro-nutrient limitation cannot be discounted as possible triggers for gamete production and sexuality. Both *P. depressum* and *P. steidingerae* produce small gametes with relatively clear pigmentation that were not observed to feed. In both species, fusing gamete pairs were isogamous and, in early stages of fusion, were oriented perpendicularly with ventral sides facing. The significance of the different thecal plate morphologies among the small cells of *P. depressum* is unknown. The two morphotypes may both be gametes, and gamete fusion may not be truly isogamous. Alternatively, one morphotype may be that of gametes, and the other that of early stage planozygotes, the result of recent gamete fusion.

In both *P. depressum* and *P. steidingerae*, sexual process appeared to be homothallic, occurring in presumptively clonal cultures. Given the similarity in the gross morphology of the vegetative cells and planozygotes within both species, however, a diploid sexual stage could have been confused with a haploid vegetative cell and used to create a culture. In live cells, nuclear features were not visible and the number of longitudinal flagella was difficult to discern and was not checked at the time of isolation. Thus, there was a chance that a culture started from a single cell may have been composed of two compatible mating types. Cultures of *P. depressum* and *P. steidingerae* started from single cells had very low survival rates relative to cultures created with multiple cells. One might speculate that those cultures founded using a single diploid cell might have had a better chance for survival, and that the cultures used in this study were not truly clonal.

Casual observations of *P. steidingerae* cultures suggested that hypnozygote production was higher and more rapid in non-clonal cultures or out-crosses. Others have documented significant

differences in hypnozygote production depending upon parental strains crossed (Figueroa and Bravo 2005), although in that case *Gymnodinium nolleri* was not homothallic. A ''preference'' rather than a requirement for heterothallism would appear to be a useful strategy for an organism in the field, allowing for maximal genetic recombination, but not precluding self-crossing and encystment when necessary for survival. Alternatively, if cultures presumed to be clonal had been founded using a diploid cell, with subsequent dominance of one mating type, this could explain the lower number of cysts in self-crosses.

Nuclear cyclosis. Meiosis in dinoflagellates is poorly characterized, but is believed to be associated with the process of nuclear cyclosis, a slow swirling of the nuclear contents often followed by cell division (von Stosch 1972). Nuclear cyclosis has been documented in different sexual life-history stages in a small number of autotrophic and heterotrophic dinoflagellates, occurring in the planozygote, zygotic division cyst, hypnozygote, or planomeiocyte (Parrow and Burkholder 2004; for reviews, see Pfiester and Anderson 1987).

In *P. steidingerae*, nuclear cyclosis appears to occur in the planomeiocyte, just before the first division. Only one protargol-stained planomeiocyte was observed to support this hypothesis, and no observations of nuclear cyclosis were made in live cells, so this premise should be considered preliminary. The nuclear morphology in the protargol-stained specimen was consistent with the morphology described for the ''Knäuel'' stage in *Ceratium* species undergoing meiosis (von Stosch 1972). Like protargol-stained specimens of *G. uncatenum* in the process of meiosis, the specimen of *P. steidingerae* had an enlarged nucleus with grainy, stained chromosomes and a single large nucleolus (Coats et al. 1984). Nuclear cyclosis was observed in a live planozygote of *P. depressum* (Bailey) Balech. In *P. depressum,* protargol-stained specimens were observed that had two trailing flagella and contained a greatly enlarged nucleus stretched across the width of the cell with grainy staining of the chromosomes and a single, large, round nucleolus in the center of the nucleus. In such specimens, the nucleus was oriented perpendicular to the longitudinal axis of the cell, unlike the obliquely oriented nucleus of a dividing cell. The similarity of the stained nucleus in the *P. steidingerae* planomeiocyte 72 d after germination to *P. depressum* specimens undergoing meiosis supports the preliminary finding that nuclear cyclosis occurs in the planomeiocyte stage in *P. steidingerae*.

Species identification. Molecular analysis of the D1–D6 region of the LSU rDNA of cells in culture confirmed that life history stages with divergent gross morphology and plate tabulation were indeed the same species. Given that all species descriptions for *Protoperidinium* spp. have been made from field specimens, morphologically distinct life-cycle stages may have been classified as separate species, as was the case with the small male gametes of *Ceratium* spp. Schrank that were assigned to the subgenus *Tripoceratium* before the sexual cycle of *Ceratium* was understood (von Stosch 1964, 1973).

Vegetative cells and cysts of *P. steidingerae* may be easily confused with the cells and cysts of *Protoperidinium oblongum* (Aurivillius) Parke and Dodge and *Protoperidinium oceanicum* (Vanhoffen) Balech if thecal plate morphology is not examined. The original description of the *P. oblongum* cyst (Wall and Dale 1968) may actually be a description of the cyst of *P. steidingerae*. The cysts in the original description were isolated from sediments in Woods Hole, MA, the same region where we collected *P. steidingerae* from the surface waters. The cysts described in the previous work had the same morphology and archeopyle type as those produced in our cultures. The cells that germinated from those cysts were called *P. oblongum* var. *latidorsale*, and, although Wall and Dale (1968) did not fully describe the thecal plate structure, their specimens did have a single intercalary plate like the species later named *P. steidingerae* (Balech 1979) instead of the three intercalary plates of *P. oblongum* (Dodge 1982). Recent molecular phylogenetic analysis establishes that *P. oblongum* and *P. steidingerae* are indeed separate species (Gribble and Anderson 2006). The morphology of the *P. oblongum* cyst should be confirmed, as it may be very similar to that of *P. steidingerae*, and extra care must be taken in field studies to discriminate both the cells and cysts of these two species.

Protoperidinium steidingerae may be the same species as both *Protoperidinium novella* and *Protoperidinium conicinna*, recently established and placed into a new subgenus, *Testeria* (Faust 2006). The SEM images presented for these two species showed the same thecal plate morphology as that of *P. steidingerae*. *Protoperidinium novella* and *P. conicinna* were separated from one another based only on cell size, ranging from 98 to 116 μm long by 62–75 μm wide and 103–137 μm long by 52–67 μm wide, respectively (Faust 2006). These cell sizes are easily encompassed in the range of sizes of the different life-history stages of *P. steidingerae* found in this study.

The gametes of *P. depressum* may have been previously mistaken for a separate species of *Protoperidinium*. Abé (1981) established the species *Protoperidinium consimilis*, which is of the same size, shape, and thecal plate morphology as the gametes of *P. depressum* described here. Understanding the morphologies of different life-history stages is also important for understanding the results of ecological and laboratory studies. Formation of ''small cells'' by *Protoperidinium* has been described in laboratory grazing studies and attributed to food limitation in culture (Jeong 1995). The results of the current study suggest that those smaller cells may have been incompletely developed daughter cells and/or sexual stages. Establishing cultures and combining molecular techniques with morphological analysis whenever possible may aid in accurate species identification.

Conclusions. This study reveals for the first time the details of asexual and sexual cycles in a species of *Protoperidinium*. Many aspects of the life histories of *P. steidingerae* and *P. depressum* remain uncharacterized, however. In particular, the triggers for sexuality are unknown for these species, and additional, unidentified stages may exist. Understanding the environmental cues leading to the sexual cycle and encystment will help to predict the dynamics of these species in the plankton. The life histories of additional species of *Protoperidinium* should be examined to determine how well conserved the characteristics of the life-cycle are among members of this diverse genus.

ACKNOWLEDGMENTS

We thank the Marine Institute of Ireland and Captain Kenneth Houtler of the Woods Hole Oceanographic Institution for sample collection. Thank you to Malte Elbrächter for assistance with identification of *P. steidingerae*. Thank you to Matthew Parrow for helpful suggestions for creating chambers for single cell culture using 96-well plates. Thank you to Rebecca Gast and Sonya Dyhrman for microscope and camera use, and to Jane Doucette for assistance with life history diagrams. The Comer Foundation, the Woods Hole Oceanographic Institution Biology Department Education Fund, and the Carroll Wilson Award from the MIT Entrepreneurship Society provided funding for this work.

LITERATURE CITED

Abé, T. H. 1981. Studies on the Family Peridiniidae: An Unfinished Monograph of the Armoured Dinoflagellata. Academia Scientific Book, Inc., Tokyo, Japan. 409 p.

Anderson, D. M., Kulis, D. M. & Binder, B. J. 1984. Sexuality and cyst formation in the dinoflagellate *Gonyaulax tamarensis*: cyst yield in batch cultures. *J. Phycol.*, **20**:418–425.

Balech, E. 1974. El genero *Protoperidinium* Bergh, 1881 (*Peridinium* Ehrenberg, 1831, Partim). *Rev. Mus. Arg. Cien. Nat. ''B. Rivadavia'' Inst. Nacional Invest. Cien. Nat.*, **4**:1–79.

Balech, E. 1979. Tres Dinoflagelados nuevos o interesantes de aguas Basileñas. *Bolm Inst. Oceanogr., S. Paulo*, **28**:55–64.

Buskey, E. J., Coulter, C. J. & Brown, S. L. 1994. Feeding, growth and bioluminescence of the heterotrophic dinoflagellate *Protoperidinium huberi*. *Mar. Biol.*, **121**:373–380.

Coats, D. W. & Heinbokel, J. F. 1982. A study of reproduction and other life-cycle phenomena in planktonic protists using an acridine orange fluorescence technique. *Mar. Biol.*, **67**:71–79.

Coats, D. W., Tyler, M. A. & Anderson, D. M. 1984. Sexual processes in the life-cycle of *Gyrodinium uncatenum* (Dinophyceae): a morphogenic overview. *J. Phycol.*, **20**:351–361.

Daugbjerg, N., Hansen, G., Larsen, J. & Moestrup, Ø. 2000. Phylogeny of some of the major genera of dinoflagellates based on ultrastructure and partial LSU rDNA sequence data, including the erection of three new genera of unarmoured dinoflagellates. *Phycologia*, **39**:302–317.

Dodge, J. D. 1982. Marine Dinoflagellates of the British Isles. Her Majesty's Stationery Office, London. 303 p.

Faust, M. A. 2006. Creation of the subgenus *Testeria* Faust subgen. nov. *Protoperidinium* Bergh from the SW Atlantic Ocean: *Protoperidinium novella* sp. nov. and *Protoperidinium conicinna* sp. nov. Dinophyceae. *Phycologia*, **45**:1–9.

Figueroa, R. I. & Bravo, I. 2005. A study of the sexual reproduction and determination of mating type of *Gymnodinium nolleri* (Dinophyceae) in culture. *J. Phycol.*, **41**:74–83.

Fritz, L. & Triemer, R. E. 1985. A rapid simple technique utilizing Calcofluor white M2R for the visualization of dinoflagellate thecal plates. *J. Phycol.*, **21**:662–664.

Gaines, G. & Taylor, F. J. R. 1984. Extracellular digestion in marine dinoflagellates. *J. Plankton Res.*, **6**:1057–1062.

Gribble, K. E. & Anderson, D. M. 2006. Molecular phylogeny of the heterotrophic dinoflagellates, *Protoperidinium*, *Diplopsalis*, and *Preperidinium* (Dinophyceae), inferred from LSU ribosomal DNA. *J. Phycol.*, **42**:1081–1095.

Guillard, R. R. L. 1975. Culture of phytoplankton for feeding marine invertebrates. *In*: Smith, W. L. & Chanley, M. H. (ed.), Culture of Marine Invertebrates. Plenum Publishing Corporation, New York, NY. p. 26–60.

Jacobson, D. M. & Anderson, D. M. 1986. Thecate heterotrophic dinoflagellates: feeding behavior and mechanisms. *J. Phycol.*, **22**:249–258.

Jacobson, D. M. & Anderson, D. M. 1993. Growth and grazing rates of *Protoperidinium hirobis* Abé, a thecate heterotrophic dinoflagellate. *J. Plankton Res.*, **15**:723–736.

Jeong, H. J. 1995. The interactions between microzooplanktonic grazers and dinoflagellates causing red tides in the open coastal waters off Southern California. Oceanography, University of California, San Diego, CA. 139 p.

Jeong, H. J. 1996. The predation impact by the heterotrophic dinoflagellate *Protoperidinium* cf. *divergens* on copepod eggs in the presence of co-occurring phytoplankton prey. *J. Oceanol. Soc. Korea. Seoul*, **31**:144–149.

Jeong, H. J. & Latz, M. I. 1994. Growth and grazing rates of the heterotrophic dinoflagellates *Protoperidinium* spp. on red tide dinoflagellates. *Mar. Ecol. Prog. Ser.*, **106**:173–185.

Kokinos, J. P. & Anderson, D. M. 1995. Morphological development of resting cysts in cultures of the marine dinoflagellate *Lingulodinium polyedrum* (= *L. machaerophorum*). *Palynology*, **19**:143–166.

Menden-Deuer, S., Lessard, E. J., Satterberg, J. & Grünbaum, D. 2005. Growth rates and starvation survival of three species of the pallium-feeding, thecate dinoflagellate genus *Protoperidinium*. *Aquat. Microb. Ecol.*, **41**:145–152.

Montagnes, D. J. S. & Lynn, D. H. 1993. A quantitative protargol stain (QPS) for ciliates and other protists. *In*: Kemp, P. F., Sherr, B. F., Sherr, E. B. & Cole, J. B. (ed.), Handbook of Methods in Aquatic Microbial Ecology. Lewis Publishers, CRC. Press Inc., Boca Raton, FL. p. 229–240.

Naustvoll, L. J. 2000. Prey size spectra and food preferences in thecate heterotrophic dinoflagellates. *Phycologia*, **39**:187–198.

Parrow, M. W. & Burkholder, J. M. 2004. The sexual life-cycles of *Pfiesteria piscicida* and cryptoperidiniopsoids (Dinophyceae). *J. Phycol.*, **40**:664–673.

Parrow, M. W., Burkholder, J. M., Deamer, N. J. & Zhang, C. 2002. Vegetative and sexual reproduction in *Pfiesteria* spp. (Dinophyceae) cultured with algae prey, and inferences for their classification. *Harmful Algae*, **1**:5–33.

Pfiester, L. A. & Anderson, D. M. 1987. Dinoflagellate reproduction. *In*: Taylor, F. J. R. (ed.), The Biology of Dinoflagellates. Botanical Monographs. Blackwell Scientific Publications, Boston, MA. p. 611–648.

Scholin, C. A., Herzog, M., Sogin, M. & Anderson, D. M. 1994. Identification of group- and strain-specific genetic markers for globally distributed *Alexandrium* (Dinophyceae). II. Sequence analysis of a fragment of the LSU rRNA gene. *J. Phycol.*, **30**:999–1011.

Thompson, J. D., Gibson, T. J., Plewniak, F., Jeanmougin, F. & Higgins, D. G. 1997. The ClustalX windows interface: flexible strategies for multiple sequence alignment aided by quality analysis tools. *Nucleic Acids Res.*, **22**:4673–4680.

von Stosch, H. A. 1964. Zum problem der sexuellen fortpflanzung in der Peridineengattung *Ceratium*. *Helgoländer wiss. Meeresunters.*, **10**:140–151.

von Stosch, H. A. 1972. La signification cytologique de la ''cyclose nucléaire'' dans le cycle de vie des Dinoflagellés. *Soc. bot. Fr., Mémoires*. p. 201–212.

von Stosch, H. A. 1973. Observations on vegetative reproduction and sexual life-cycles of two freshwater dinoflagellates, *Gymnodinium pseudopalustre* Schiller and *Woloszynskia apiculata* sp. nov. *Br. Phycol. J.*, **8**:105–134.

Wall, D. & Dale, B. 1968. Modern dinoflagellate cysts and evolution of the Peridiniales. *Micropaleontology*, **14**:265–304.

Received: 08/07/08, 9/18/08; accepted: 08/19/08